A genome-wide search for genetic influences and biological pathways related to the brain's white matter integrity

Lorna M. Lopez[a,b,1,*], Mark E. Bastin[a,c,d,e], Susana Muñoz Maniega[a,c,d], Lars Penke[a,b], Gail Davies[b], Andrea Christoforou[f,g], Maria C. Valdés Hernández[a,c,d], Natalie A. Royle[a,c,d], Albert Tenesa[h,i], John M. Starr[a,j], David J. Porteous[a,k], Joanna M. Wardlaw[a,c,d], Ian J. Deary[a,b]

[a] Centre for Cognitive Ageing and Cognitive Epidemiology, The University of Edinburgh, Edinburgh, UK
[b] Department of Psychology, The University of Edinburgh, Edinburgh, UK
[c] Scottish Imaging Network, A Platform for Scientific Excellence (SINAPSE) Collaboration, Department of Clinical Neurosciences, The University of Edinburgh, Edinburgh, UK
[d] Brain Research Imaging Centre, Department of Clinical Neurosciences, The University of Edinburgh, Edinburgh, UK
[e] Division of Health Sciences (Medical Physics), The University of Edinburgh, Edinburgh, UK
[f] Dr Einar Martens Research Group for Biological Psychiatry, Department of Clinical Medicine, University of Bergen, Bergen, Norway
[g] Center for Medical Genetics and Molecular Medicine, Haukeland University Hospital, Bergen, Norway
[h] Institute of Genetics and Molecular Medicine, MRC Human Genetics Unit, Edinburgh, UK
[i] The Roslin Institute, Royal (Dick) School of Veterinary Studies, The University of Edinburgh, Roslin, UK
[j] Geriatric Medicine Unit, The University of Edinburgh, Royal Victoria Hospital, Edinburgh, UK
[k] Medical Genetics Section, The University of Edinburgh, Molecular Medicine Centre, Western General Hospital, Edinburgh, UK

Abstract

A genome-wide search for genetic variants influencing the brain's white matter integrity in old age was conducted in the Lothian Birth Cohort 1936 (LBC1936). At ~73 years of age, members of the LBC1936 underwent diffusion MRI, from which 12 white matter tracts were segmented using quantitative tractography, and tract-averaged water diffusion parameters were determined (n = 668). A global measure of white matter tract integrity, g_{FA}, derived from principal components analysis of tract-averaged fractional anisotropy measurements, accounted for 38.6% of the individual differences across the 12 white matter tracts. A genome-wide search was performed with g_{FA} on 535 individuals with 542,050 single nucleotide polymorphisms (SNPs). No single SNP association was genome-wide significant (all $p > 5 \times 10^{-8}$). There was genome-wide suggestive evidence for two SNPs, one in *ADAMTS18* ($p = 1.65 \times 10^{-6}$), which is related to tumor suppression and hemostasis, and another in *LOC388630* ($p = 5.08 \times 10^{-6}$), which is of unknown function. Although no gene passed correction for multiple comparisons in single gene-based testing, biological pathways analysis suggested evidence for an over-representation of neuronal transmission and cell adhesion pathways relating to g_{FA}.
© 2012 Elsevier Inc. All rights reserved.

Keywords: Genome-wide association study; White matter; MRI; Diffusion; Tractography

1. Introduction

A new era in brain imaging genetics is beginning, based on the availability of quantitative structural MRI methods and the genotyping of hundreds of thousands of genetic markers on a genome-wide scale. Combining genetic data with imaging modalities such as diffusion MRI (Beaulieu, 2002) and tractography, which measures the mobility of water molecules *in vivo* and provides metrics of white

[1] Lorna M. Lopez has previously published under her maiden name Lorna M. Houlihan.

* Corresponding author at: Centre for Cognitive Ageing and Cognitive Epidemiology, The University of Edinburgh, 7 George Square, Edinburgh, EH8 9JZ, UK. Tel.: +44 (0) 131 6508495; fax: +44 (0) 131 6511771.

    E-mail address: lorna.lopez@ed.ac.uk (L.M. Lopez).

matter integrity in specific pathways (Behrens et al., 2007), may provide valuable insights into the genetic influences on large-scale axonal development, synaptic connectivity, and fiber architecture, and ultimately inform on the biological basis of brain disorders (Hibar et al., 2011a).

Studies of twins have shown that aspects of brain structure and function are highly heritable throughout the lifespan (Gilmore et al., 2010; Kremen et al., 2010; Rimol et al., 2010; Schmitt et al., 2010). Three heritability studies are noteworthy. First, in 92 identical and fraternal twins, additive genetic factors explained between 75% and 90% of the variance in white matter fractional anisotropy (FA) in bilateral frontal, bilateral parietal, and left occipital lobes (Chiang et al., 2009). Second, in 15 monozygotic and 18 dizygotic twin pairs of elderly men, additive genetic contributions explained 67% and 49% of the total variance in corpus callosum FA, respectively (Pfefferbaum et al., 2001). Third, a family study of 467 healthy individuals from 49 Mexican-American families showed a significant heritability for whole brain-averaged FA ($h^2 = 0.52$, $p = 10^{-7}$); that is, more than 50% of the individual differences in FA were explained by additive genetic factors (Kochunov et al., 2010).

Despite this evidence of a genetic contribution to differences in white matter integrity, the specific genetic causes remain largely unknown. Searches for these genetic influences have so far focused on candidate genes and have had limited success in identifying genes linked to white matter structure in healthy individuals (Thompson et al., 2010). One candidate gene study investigated the effects of the gene encoding the brain-derived neurotrophic factor (BDNF) (Chiang et al., 2011a). In this study of 258 twins, a common genetic polymorphism within *BDNF* accounted for ~15% of the variance in FA in major white matter fiber tracts, and this finding was replicated in a study of 455 twins. A second study investigated healthy younger and older individuals and found a general reduction of FA in carriers of the apolipoprotein E (*APOE* gene) $\varepsilon 4$ allele (Heise et al., 2011). A third candidate gene association study in older individuals demonstrated genetic association between a functional genetic polymorphism in the β_2-adrenergic receptor gene (*ADRB2*) and FA measures of the left arcuate fasciculus and the splenium of the corpus callosum (Penke et al., 2010b). Further regions on chromosomes 15q25 and 3q27 have also been linked with white matter circuitry and brain structure in the aforementioned Mexican-American family study (Kochunov et al., 2010). An alternative to the candidate gene approach is the hypothesis-free, genome-wide association study strategy. Genome-wide association studies have been useful for identifying many genes in non–brain-related human traits (Houlihan et al., 2010; WTCCC, 2007). However, effectively linking high-throughput single nucleotide polymorphism (SNP) data to large-scale imaging data remains a challenging task.

Here, we report the first genome-wide association study, using 542,050 SNPs, of a general factor of white matter integrity, which we call g_{FA}. It was determined using diffusion MRI tractography data collected from the Lothian Birth Cohort 1936 (LBC1936), a large group of relatively healthy older people in their eighth decade (Deary et al., 2007; Wardlaw et al., 2011). Previously, in a subsample of the LBC1936, we found that the integrity of different white matter tracts, as indicated by tract-averaged FA, was strongly positively correlated, showing that individuals with lower integrity in one white matter tract tended to have lower integrity in other tracts as well, making white matter tract integrity a brain-wide property (Penke et al., 2010a). A derived general white matter integrity factor, g_{FA}, captured the common integrity variance across tracts. The present study searches genome-wide for genetic associations to this general factor of brain white matter integrity and takes a tiered approach to investigate genetic influences on $g_{FA,}$ at the SNP level, at the gene level, and at the level of biological pathways.

2. Methods

2.1. Subjects

The LBC1936 consists of community-dwelling, relatively healthy individuals (Deary et al., 2007) who were all born in 1936 and participated in the Scottish Mental Survey 1947 (SMS1947) (Scottish Council for Research in Education Mental Survey Committee, 1949). From 2008 to 2010 at a mean age of ~73 years, 866 (418 female) LBC1936 individuals undertook medical, genetic, and cognitive testing, alongside additional investigations including detailed brain MRI (Wardlaw et al., 2011). Tractography data were available for 668 individuals. Of these 668, the study sample with nonmissing tractography and genome-wide genotype data comprised 535 individuals (256 females) with a mean age of 72.7 (SD = 0.74) years. All individuals were healthy, right-handed, and showed no evidence of cognitive pathology on self-reported medical history or on a brief dementia screening test; Mini-Mental State Examination (MMSE) scores were ≥ 24 (Folstein et al., 1975). The study was approved by the Lothian (REC 07/MRE00/58) and Scottish Multicenter (MREC/01/0/56) Research Ethics Committees, and all subjects gave written informed consent.

2.2. Diffusion MRI protocol

All MRI data were acquired at the Brain Research Imaging Centre, associated with the Wellcome Trust Clinical Research Facility, The University of Edinburgh, using the same GE Signa Horizon HDxt 1.5-T clinical scanner (General Electric, Milwaukee, WI, USA) equipped with a self-shielding gradient set (33 mT/m maximum gradient strength) and manufacturer-supplied eight-channel phased-array head coil. The diffusion MRI protocol consisted of seven T_2-weighted (b = 0 seconds/mm^2) and sets of diffu-

sion-weighted (b = 1000 seconds/mm^2) axial single-shot spin-echo echo-planar (EP) volumes acquired with diffusion gradients applied in 64 noncollinear directions (Jones et al., 2002). Seventy-two contiguous axial slices of 2-mm thickness were acquired with a field of view of 256 × 256 mm and matrix size of 128 × 128, giving a resolution of 2 × 2 × 2 mm. Repetition time was 16.5 seconds and echo time was 95.5 ms, producing a total scan time of approximately 20 minutes.

2.3. Diffusion tensor processing

Using FMRIB Software Library (FSL) tools (fmrib.ox.ac.uk/fsl), the diffusion MRI data were preprocessed to extract the brain (Smith, 2002) and remove bulk patient motion and eddy current-induced artifacts by registering the diffusion weighted to the first T$_2$-weighted EP volume for each subject (Jenkinson and Smith, 2001). Mean FA volumes were created using DTIFIT. Brain connectivity data for the tractography analysis were generated using BedpostX/ProbTrackX run with its default parameters of a two-fiber model per voxel and 5000 probabilistic streamlines for each tract, with a fixed separation distance of 0.5 mm between successive points (Behrens et al., 2007). Probabilistic neighborhood tractography, as implemented in the TractoR package for fiber tracking and analysis (code.google.com/p/tractor), was used to segment the same fasciculus in each subject from single seed point tractography output using probabilistic tract shape modeling (Bastin et al., 2010; Clayden et al., 2007, 2009b). In this method, the optimum tractography seed point was determined by estimating the best-matching tract from a series of candidate tracts generated from a 7 × 7 × 7 neighborhood of voxels placed around a voxel transferred from standard to native space against a reference tract that was derived from a digital human white matter atlas (Muñoz Maniega et al., 2008). The topological tract model was also used to reject any false-positive connections (Clayden et al., 2009a), thereby significantly improving tract segmentation (Bastin et al., 2010). For each subject, the seed point that produced the best-match tract to the reference was determined for 12 major white matter pathways, specifically genu and splenium of corpus callosum, bilateral anterior thalamic radiations, cingulum cingulate gyri, and arcuate, uncinate, and inferior longitudinal fasciculi. The resulting tractography masks were then applied to each subject's FA volume to generate tract-averaged FA values for each fiber pathway. To ensure that the segmented tracts were anatomically plausible representations of the fasciculi of interest, a researcher (S.M.M.) visually inspected all masks blind to the other study variables and excluded tracts with aberrant or truncated pathways. In general, probabilistic neighborhood tractography was able to segment the 12 tracts of interest reliably in the majority of subjects (n = 668), with tracts that did not meet quality criteria (truncation or failed to follow expected path) ranging from 0.3% for the splenium of the corpus callosum to 16% for the left anterior thalamic radiation, with a mean of 5%.

2.4. Genome-wide association data

A detailed description of the genome-wide association study methods used in the LBC1936 is available elsewhere (Houlihan et al., 2010). In brief, genotyping was performed using an Illumina Human 610-Quadv1 chip (Illumina, Inc., San Diego, CA, USA) on blood-extracted DNA. Standard quality control measures were applied including the following thresholds: call rate ≥ 0.98, minor allele frequency ≥ 0.01, and Hardy–Weinberg equilibrium test with $p \geq 0.001$. The final number of SNPs was 542,050.

2.5. Statistical analyses

2.5.1. Imaging phenotypes

A general factor of white matter integrity, g$_{FA}$, was derived using principal components analysis (PCA), as previously described in a pilot sample (Penke et al., 2010a), with the following updates. PCA was applied to the tract-averaged FA values measured from the 12 segmented tracts. Up to three missing values per individual were imputed by replacing the missing values by the mean value for that specific white matter tract. A clear one-component solution was demonstrated with the first unrotated principal component accounting for 38.60% of the variance. Figure 1 shows that all 12 tracts showed substantial positive loadings on the component (mean loading = 0.617; range, 0.352–0.701). The principal phenotype used in this study, g$_{FA}$, was the score on the first unrotated principal component of the PCA analysis of the tract-averaged FA values of the 12 white matter pathways (mean = 0, standard deviation = 1), with a high value of g$_{FA}$ indicating elevated FA across all tracts.

2.5.2. Association analysis

Association between g$_{FA}$ and genome-wide SNPs was tested by linear regression analysis in PLINK version 1.07 (pngu.mgh.harvard.edu/~purcell/plink), covarying for gender and age in days at the time of brain imaging, under an additive genetic model (Purcell et al., 2007). To test independence of the top associated SNPs (rs7192208 and rs946836), conditional analysis was performed in PLINK. This includes the allelic dosage of the specified SNPs as a covariate in a linear regression analysis. If other SNPs are still significant after this analysis, this would suggest that these SNPs are having an effect on the trait, independent of the conditioned SNPs. Quantile-quantile (QQ) plots and Manhattan plots of the genome-wide association analysis were visualized using WGAviewer (Ge et al., 2008) and an R script "ggplot2" (gettinggeneticsdone.blogspot.com). To calculate the genotype means in PASW Statistics version 17.0.2 (SPSS Inc., Chicago, IL, USA), the phenotype was first regressed for age and sex as covariates (mean = 0, standard deviation = 1). The genotyping clusters of the top associated hits were visually inspected to check for errone-
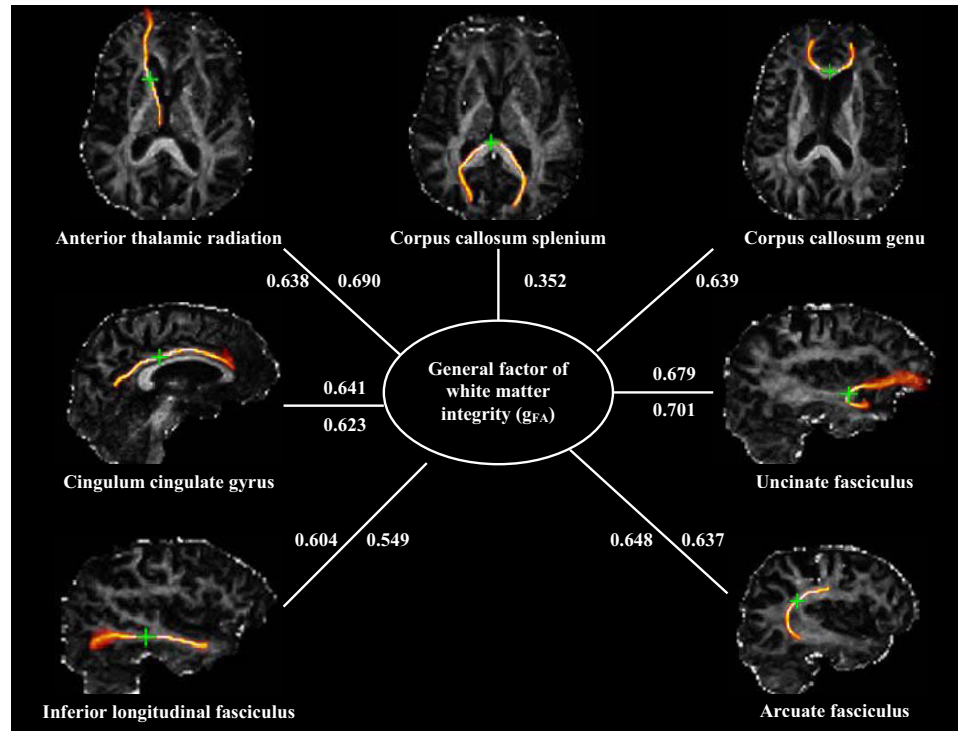
Fig. 1. Illustration of the general factor of white matter integrity, g_{FA}. Brain images show white matter tract segmentations obtained in one representative participant for 12 tracts, namely, genu and splenium of the corpus callosum, bilateral anterior thalamic radiations, cingulum cingulate gyri, and arcuate, uncinate, and inferior longitudinal fasciculi. Seed points are marked with a green cross, and tracts are projected into the plane of the seed point. The statistics on the lines are the factor loadings of the average FA values of the tracts on the latent white matter integrity factor. For bilateral tracts, both left and right factor loadings are provided to the left or top, and right or bottom, of the line, respectively. For interpretation of the references to color in this figure legend, the reader is referred to the Web version of this article.

ous genotype calling in Illumina Genomestudio version 1.0.2.20706 (illumina.com).

2.5.3. Genetic investigations

Genes and predicted genes (expressed sequence tags) close to significant SNPs were localized through the UCSC genome browser (Kent et al., 2002) (genome.ucsc.edu). Gene functions and known associations with disease were explored using the Online Mendelian Inheritance in Man database (OMIM; ncbi.nlm.nih.gov/omim), GeneCards (genecards.org), Genetic Association Database (geneticassociationdb.nih.gov), NextBio (nextbio.com), SNPexp (app3.titan.uio.no/biotools/help.php?app=snpexp), and SNP express (Heinzen et al., 2008) (people.chgv.lsrc.duke.edu/~dg48//SNPExpress/index.php).

2.5.4. Gene-based analyses

Gene-based analysis was performed using the VErsatile Gene-based Association Study (VEGAS) test (Liu et al., 2010) (gump.qimr.edu.au/VEGAS). This gene-based test works by summarizing the evidence for association to g_{FA} on a per-gene basis by considering the p-value of all SNPs within 17,787 autosomal genes according to positions on the UCSC Genome Browser hg18 assembly (including $\pm$ 50 kb up- and downstream of the gene from the 5′ and 3′ untranslated regions), while accounting for linkage disequilibrium between markers by using simu-

lations from the multivariate normal distribution and the number of SNPs per gene. The significance threshold applied was $p < 2.8 \times 10^{-6}$ ($\approx 0.05/17{,}787$). Published candidate genes previously associated with the white matter of the brain measured by FA in healthy individuals were examined for associations with g_{FA} in the LBC1936 using VEGAS.

2.5.5. Biological pathway analysis

To extract biological meaning from the large list of genes suggestively associated with g_{FA}, biological pathway analysis was performed using Web-based Gene Set Enrichment Analysis Toolkit (WebGestalt2) (Duncan et al., 2010; Zhang et al., 2005). A gene list from VEGAS analysis ($p < 0.01$, n = 177 genes) was uploaded. Gene ontology annotations were found for 173 genes. An enrichment analysis for the gene ontology categories was performed using the recommended settings: Statistical Method was the hypergeometric test; Multiple Test Adjustment was Benjamini and Hochberg method (Benjamini and Hochberg, 1995); the significance level for the adjusted p-value was 0.05; the minimum number of genes for a category was 2. The results are represented by an enriched directed acyclic graph (DAG) and in tabular form.

2.5.6. Clustering of functional annotation

To search for biological terms and functions that are specifically enriched in genetic associations with white matter and to group these biological terms according to similar functionality, analysis was performed using DAVID (the Database for Annotation, Visualization, and Integrated Discovery), a data-mining integrated environment of bioinformatics resources (Huang et al., 2009). A gene list was uploaded, based on the VEGAS analyses ($p < 0.01$, n = 177 genes). Functional annotation clustering analysis on these gene lists using Gene Ontology (GO) terms (GOTERM_BP_FAT, GOTERM_CC_FAT, GOTERM_MF_FAT) and pathways (BBID, BIOCARTA, KEGG) was performed. The highest clustering stringency was used, as this generates fewer functional groups, with more tightly associated genes in each group. The number in each gene list tested with corresponding DAVID IDs was 127 for VEGAS. Within each annotation cluster is a group of terms with similar biological meaning due to sharing similar gene members. The authors advise that clusters with an enrichment score of 1.3 or greater should be given further attention, as this is equivalent to non-log scale of $p = 0.05$.

2.5.7. Statistical power

Formal calculations were performed to establish the statistical power available in this study to detect genetic variants associated with g_{FA}. These were estimated using the variance component quantitative trait loci association module in the genetic power calculator (Purcell et al., 2003). With a sample size of 535, this study has 80% power to detect an additive effect of a causal variant, in linkage disequilibrium D' = 1 of a marker with a minor allele frequency of 0.25 (mean minor allele frequency of the 542,050 SNPs in this study), accounting for 7% of the variance, at type 1 error rate adjusted for multiple testing (p-value $\leq 5 \times 10^{-8}$). This is adequate power to detect the effect sizes previously associated with white matter integrity, for example, *BDNF* (Chiang et al., 2011a), but has reduced power to detect effect sizes less than 7%.

3. Results

3.1. Genome-wide association study

The QQ plot (Fig. 2a) shows no evidence of population stratification, as the observed line does not deviate from that which is expected (red line), and the lambda value suggests no inflation of association signals in accordance with random expectation ($\lambda = 1.0092$). A further test of population stratification was performed by checking for association between the first four components from a multidimensional scaling analysis (MDS) of the SNP data and the phenotype under investigation here, g_{FA}. The MDS analysis was carried out using the entire LBC1936 cohort, as described in Davies et al. (2011), and also using the subset of 535 individuals included in this study. There was no evidence of

an association with either set of MDS components (all p-values > 0.05), and therefore no suggestion of underlying population substructure.

Genome-wide association analysis of 542,050 SNPs with g_{FA} found no SNPs that surpassed the conventional threshold for genome-wide significance ($p < 5 \times 10^{-8}$). There were two SNPs with genome-wide support for suggestive association of $p < 1 \times 10^{-5}$ (Figs. 2b and 3, Table 1). In all, 570 SNPs were associated at a significance level $p < 1 \times 10^{-3}$ and are listed in Supplementary Table 1. The strongest association was with rs7192208 ($p = 1.65 \times 10^{-6}$). This SNP is located in an intron of the gene *ADAMTS18*. The other genome-wide suggestive association was with rs946836 ($p = 5.08 \times 10^{-6}$). This SNP is an intronic marker in a putative protein-coding gene called *LOC 388630*. The association of both SNPs with g_{FA} was independent of each other as tested by conditional analysis. Together, these two variants explain ~6% of the variance in g_{FA} when both SNPs were included in the regression model. Post hoc analysis shows that rs7192208 and rs946836 are nominally associated with almost all 12 white matter tracts (all p-values < 0.1; Supplementary Table 2). In particular, rs7192208 is most significantly associated with the left arcuate fasciculus ($p = 2.55 \times 10^{-5}$) and rs946836 ($p = 2.57 \times 10^{-5}$) with the left uncinate fasciculus. Figure 4 illustrates the clearly additive effect of both genome-wide suggestive hits on g_{FA}. For the *ADAMTS18* SNP, rs7192208, the addition of the minor allele (G) is associated with decreased g_{FA}. Conversely, for the SNP rs946836 in *LOC388630*, the addition of the minor allele (T) is associated with increased g_{FA}.

Furthermore, the association of both genome-wide suggestive SNPs with the expression of their corresponding genes, *ADAMTS18* and *LOC388630*, was tested using online resources. Of the 30 exon probes specific for *ADAMTS 18*, expression of 21 exon probes was associated with rs7192208 in brain tissue (p-values < 0.05) (Heinzen et al., 2008). Neither rs7192208 nor rs946836 was associated with *ADAMTS18* or *LOC388630*, respectively, in lymphoblastoid cell lines (SNPexp) or with peripheral blood mononuclear cell tissue (Heinzen et al., 2008). This suggests that rs7192208 influences *ADAMTS18* expression through *cis*-acting genetic regulation in the brain.

3.2. Gene-based analyses

A gene-based analysis was performed to consider associations between g_{FA} and 17,787 genes in VEGAS (Liu et al., 2010). None of the genes passed a Bonferroni threshold for significance ($p < 2.8 \times 10^{-6}$). Table 2 shows 19 top associated genes ($p < 0.001$). The most associated gene is *OR1G*, an olfactory receptor, family 1, subfamily G, member 1. Another associated gene on chromosome 17 is *OR1D2*, an olfactory receptor, family 1, subfamily D, member 2. Olfactory receptors interact with odorant molecules in the nose to initiate a neuronal response that triggers the
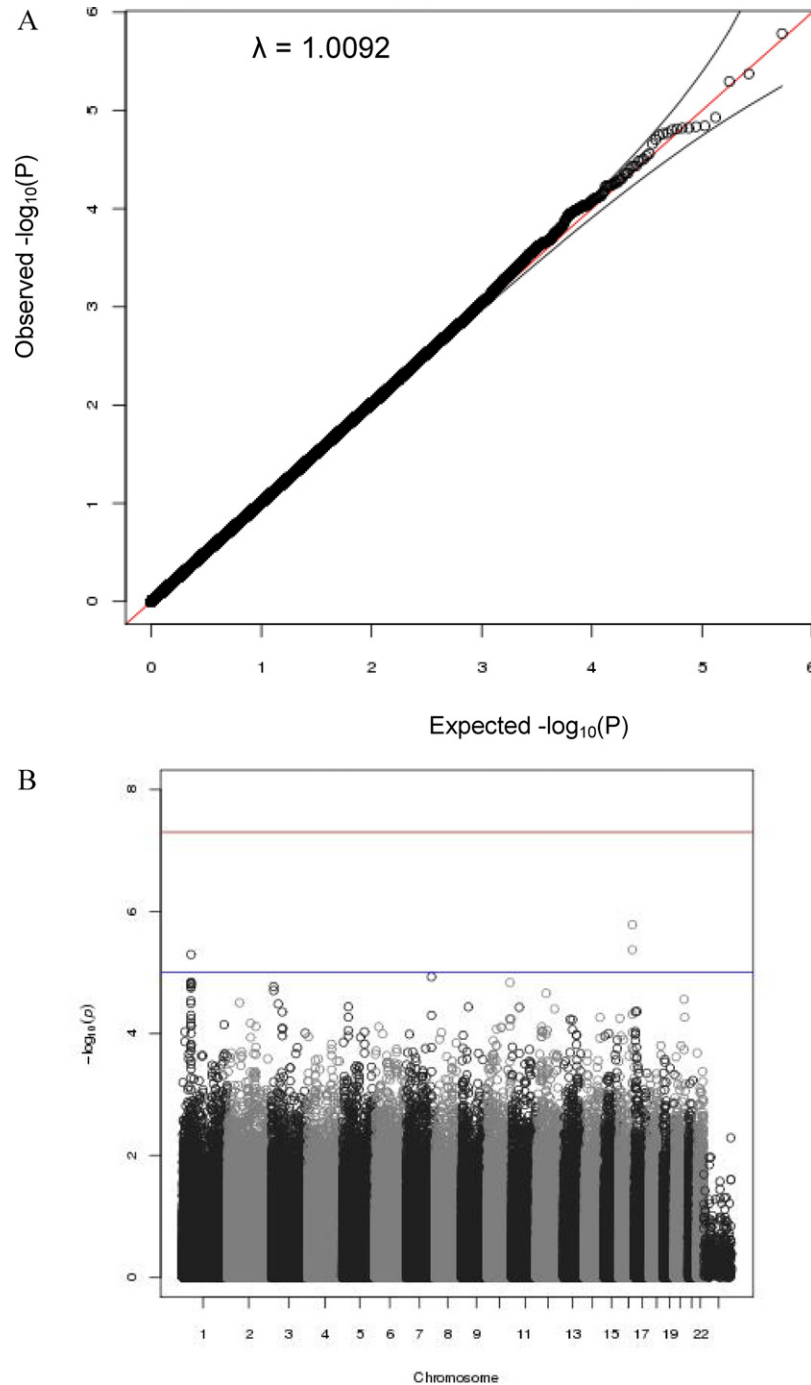
Fig. 2. Genome-wide association study *p*-values for g_{FA}. (A) Quantile-quantile plot of the association analysis *p*-values. The black circles represent the observed data; the red line is the expectation under the null hypothesis of no association; and the black curves are the boundaries of the 95% confidence interval. The lambda value suggests no inflation of association signals in accordance with random expectation. (B) Manhattan plot. The x-axis represents the position of each chromosome from the p terminus to the q terminus. The y-axis depicts *p*-values (–log10[*p*-values]). Genome-wide significance threshold is in red (–log10[5×10^{-8}]), and suggestive threshold is in blue (−log10[1×10^{-5}]). For interpretation of the references to color in this figure legend, the reader is referred to the Web version of this article.

perception of a smell (GeneCards). Five genes on chromosome 12 (*CDK2*, *WIBG*, *SILV* now known as *PMEL*, *RAB5B*, *DGKA*; four genes are overlapping) show nominal association. These five genes are implicated in cancer but have no known influence on the brain's white matter. In all, 177 genes were nominally associated as listed in Supplementary Table 3 (*p* < 0.01). From the single SNP analysis, *ADAMTS18* shows a nominal association at the gene level (*p* = 7.87×10^{-4}), and *LOC388630* was not tested because it is a putative gene. The lack of a strong
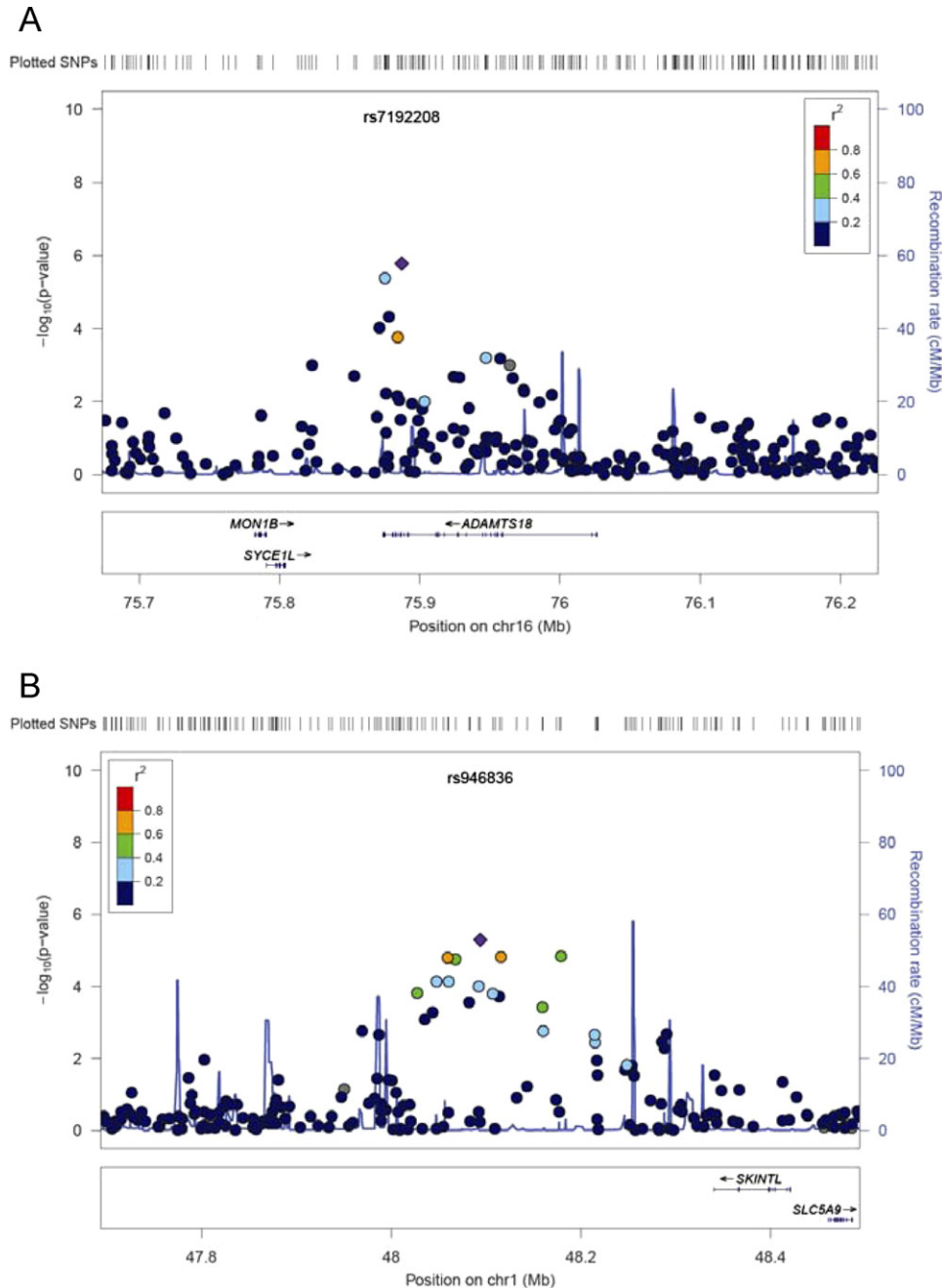
Fig. 3. Detailed view of the associated loci with g_{FA}. Markers are represented as circles (SNPs with no known function) or a diamond for the most significant SNP. Markers are placed at their chromosomal position (x-axis) and graphed based on the –log10 (*p*-values) of their association to g_{FA} (y-axis). The level of linkage disequilibrium (r^2) to the most-associated SNP labeled on the graph is represented in color using the CEU panel (Utah residents with Northern and Western European ancestry from the CEPH collection) from HapMap Phase II. The location of the genes is shown below the plots. The estimated recombination rate from HapMap samples is also shown. Images were created using LocusZoom (Pruim et al., 2010). For interpretation of the references to color in this figure legend, the reader is referred to the Web version of this article.

association of *ADAMTS18* at the gene level may be linked to the underlying genetic architecture of the gene, such that the *ADAMTS18* significant SNP (rs7192208) may be, or have a direct link to, the causal variant, and the other 102 SNPs in this large gene (~153 kb) may have diluted the gene's significance.

In the literature, variants in 13 genes have been reported in at least one study as being associated or linked with white matter integrity measured by FA in healthy individuals. Table 3 shows that only one of the 13 genes that was previously associated with white matter integrity in a pilot study of the LBC1936 remained associated, in

Table 1
Independent SNPs associated with g_{FA}

Chr	Gene	SNP	Minor allele	Major allele	N	MAF	Beta	SE	R^2	*p*-value
16	*ADAMTS18*	rs7192208	G	T	533	0.11	−0.48	0.0997	0.042	1.65×10^{-6}
1	*LOC388630*	rs946836	T	C	535	0.33	0.30	0.0651	0.038	5.08×10^{-6}

SNPs surviving the $p < 1 \times 10^{-5}$ threshold for suggestive genome-wide evidence for association with the general factor of white matter integrity. N is the sample size; MAF, the minor allele frequency; Beta, the regression coefficient of the trait value on the number of minor alleles; SE, the standard error; and R^2, the proportion of variance explained.

a gene-based test using VEGAS, with g_{FA} in this larger sample of LBC1936 participants (*ADRB2*, $p = 0.042$). Individual SNPs from candidate genes were not tested, except for the most promising candidate, owing to earlier genetic and biologically functional evidence, the Val 66Met polymorphism in *BDNF*. This was not associated with the g_{FA} in the current study (rs6265, $p = 0.73$) (Chiang et al., 2011a).

3.3. Biological pathway analysis

Pathway analysis with a gene ontology method was undertaken using WebGestalt2 on 173 genes suggestively associated with g_{FA} in the LBC1936 from gene-based VEGAS analysis ($p < 0.01$). Twenty-three gene ontology categories were found to have enriched gene numbers using all genes in the human genome as a reference. Twelve categories were under "biological process," and 11 were under "molecular function." Supplementary Fig. 1 is an enriched DAG for the enriched categories under biological process and molecular function. The enriched categories are shown in red, and their nonenriched parents are shown in black. Most of the enriched GO categories identified for this gene set were related to cell adhesion and neuronal transmission. Supplementary Table 4 shows that the most significant category was "calcium-dependent cell-cell adhesion" ($p = 1.15 \times 10^{-11}$) for cell adhesion and "synapse assembly" ($p = 5.20 \times 10^{-8}$) for neuronal transmission.

3.4. Clustering of biologically similar pathways

The genetic associations with g_{FA} were investigated for clusters or enrichment of genes with similar biological terms and functions. Genes suggestively associated with g_{FA} from VEGAS analysis (n = 177 genes, $p < 0.01$) were cross-referenced in the DAVID database and searched for enrichment of GO terms. Twenty-five clusters were generated. Supplementary Table 5 shows the five clusters with an enrichment score > 1.3, the equivalent to non-log scale of $p = 0.05$. There was a clear clustering of genes relating to the synapse (Annotation cluster 1, enrichment score 5.59) for the GO terms synaptogenesis, synapse organization, and extracellular structure organization.

4. Discussion

To date, few genome-wide association studies have been performed in brain imaging phenotypes (Hibar et al., 2011b;

Stein et al., 2010). The present study is the first genome-wide association study with detailed white matter tractography information, obtained from a large older human sample with a narrow age range. We identified genome-wide suggestive associations between an FA-based general factor of brain white matter integrity, g_{FA}, and variants in two genes, *ADAMTS18* and *LOC388630*. Gene-based analysis and biological pathway analyses showed that there is an over-representation of associated genes relating to synaptic function.

The *ADAMTS18* gene has biological functionality to suggest a potential role in the white matter of the brain (Fig. 3a). For the particular significant SNP (rs7192208), there are no previously reported genetic associations. The gene, *ADAMTS18*, is ADAM metallopeptidase with thrombospondin type 1 motif, 18 encoding a member of the ADAMTS (a disintegrin and metalloproteinase with thrombospondin motifs) protein family. The top five tissues where *ADAMTS18* is overexpressed are the cerebellar vermis, cerebellum, cerebellar hemisphere, transverse colon, and the corpus callosum (NextBio Body Atlas; nextbio.com). *ADAMTS18* is genetically associated with bone mineral density (Deng et al., 2009), and a functional epigenetic study in multiple carcinoma cell lines has shown that *ADAMTS18* is a tumor suppressor (Jin et al., 2007). *ADAMTS18* also influences platelet lysis following thrombin-induced aggregation and increases bleeding time *ex vivo* and in a mouse model, so it may "support a possible physiologic and/or therapeutic role in haemostasis" (Li et al., 2009). This role in hemostasis may be relevant for age-related white matter damage, for example, leukoaraiosis. To lend further support to *ADAMTS18*, a related gene, ADAM metallopeptidase domain 10 (*ADAM10*), has recently been correlated with both FA of the cerebral white matter and the thickness of cortical gray matter (Kochunov et al., 2011b), and is considered a potential target for neurodegenerative disorders treatment and an Alzheimer's disease candidate gene.

Little is known about the gene *LOC388630*, in which the genome-wide suggestive SNP, rs946836, on chromosome 1 lies (Fig. 3b). *LOC388630* encodes the UPF0632 protein A of unknown function. This transcript is predominantly expressed in the colon but is also expressed in the tissues of the nervous system (NextBio Body Atlas). There was no evidence to implicate neighboring genes, as rs946836 does not correlate with any neighboring genetic variant outside of *LOC388630*. rs946836 was not in linkage disequilibrium with
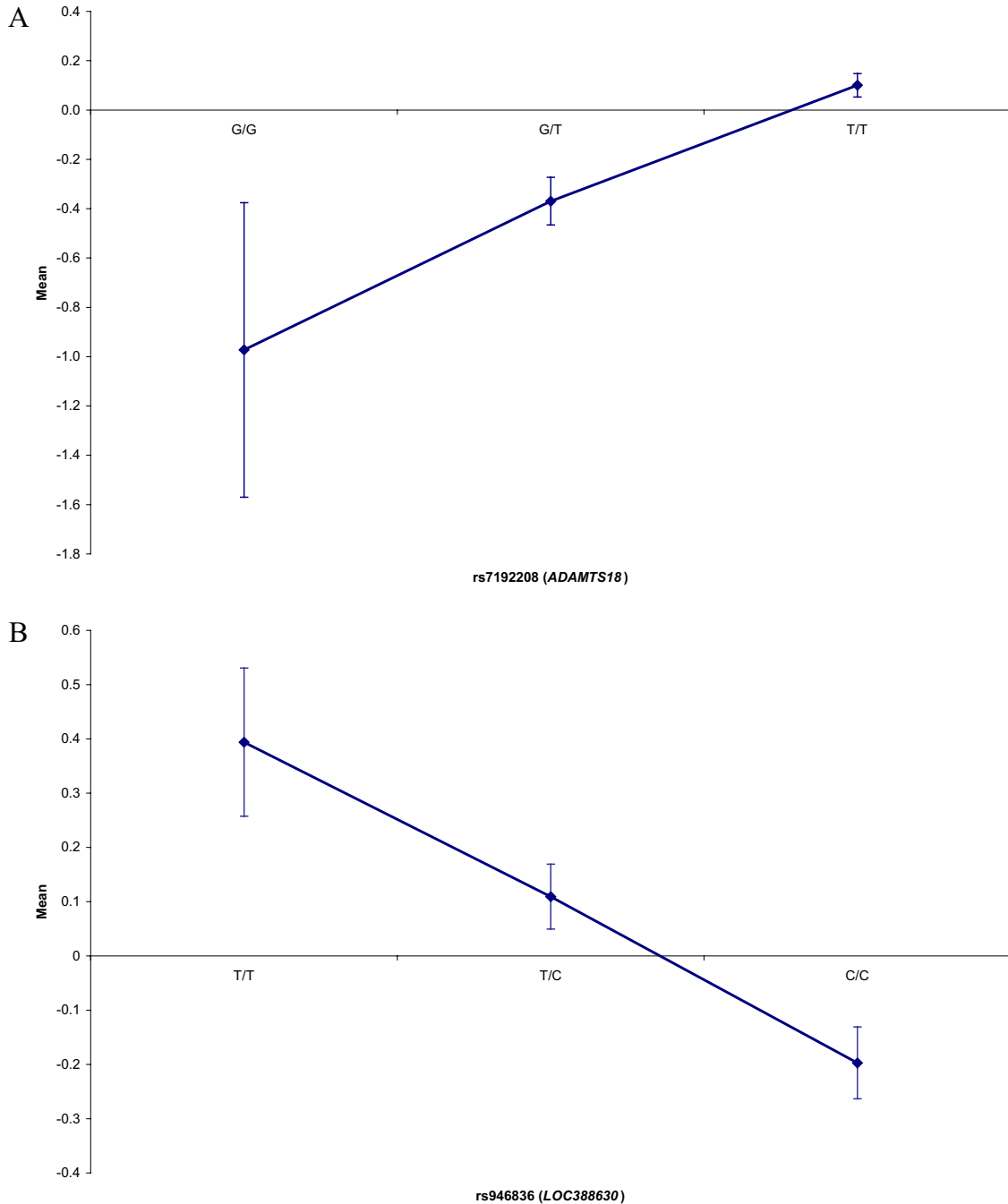
Fig. 4. The genotype means of two suggestive significant SNPs with g_{FA}: (A) rs7192208 (*ADAMTS18*) and (B) rs946836 (*LOC388630*). On the x-axis are the three genotypes; the y-axis represents g_{FA} as a standardized variable having been adjusted for age and sex (mean = 0, standard deviation = 1). The error bars are standard error on the mean. The frequencies of each genotype are GG (0.75%), GT (19.89%), and TT (79.36%) for rs7192208 and TT (9.91%), TC (45.23%), and CC (44.86%) for rs946836. For interpretation of the references to color in this figure legend, the reader is referred to the Web version of this article.

any SNP outside of *LOC388630*, other than 37 intronic SNPs in *LOC388630* ($r^2 > 0.4$) in the HapMap CEU population. Therefore, there is no known biological evidence to further imply that this gene has a role in white matter function.

The pathway analysis hints at relevant biological pathways, neuronal transmission (synaptic pathways) and cell adhesion, influencing white matter in the brain. It is known that synaptic-style release of glutamate, the brain's major excitatory neurotransmitter, occurs deep in white matter, and dysregulation of white matter synaptic transmission may play an important clinical role in multiple sclerosis, Alzheimer's disease, and other neurodegenerative diseases

Table 2
Genes showing strongest association with g_{FA} ($p < 0.001$)

Chromosome	Gene	Number of SNPs in gene ($\pm$ 50 kb)	Start position	Stop position	p-value
17	*OR1G1*	24	2,976,653	2,977,595	5.90×10^{-5}
12	*CDK2*[a]	15	54,646,822	54,652,835	6.30×10^{-5}
12	*WIBG*	12	54,581,463	54,607,964	7.20×10^{-5}
12	*SILV*[a]	14	54,634,155	54,646,093	1.37×10^{-4}
12	*RAB5B*[a]	16	54,654,128	54,674,755	1.79×10^{-4}
12	*DGKA*[a]	14	54,611,212	54,634,074	1.94×10^{-4}
10	*ACADSB*	38	124,758,418	124,807,796	2.62×10^{-4}
17	*OR1D2*	19	2,942,101	2,943,040	2.8×10^{-4}
14	*HSP90AA1*	12	101,616,827	101,675,839	3.23×10^{-4}
1	*CYP4A11*	6	47,167,432	47,179,743	4.45×10^{-4}
12	*SUOX*	15	54,677,309	54,685,576	4.47×10^{-4}
1	*CYP4B1*	35	47,037,256	47,057,608	4.87×10^{-4}
12	*SLC24A6*	13	112,220,953	112,257,308	5.04×10^{-4}
12	*TPCN1*	17	112,143,651	112,218,317	6.02×10^{-4}
16	*ADAMTS18*	103	75,873,525	76,026,512	7.87×10^{-4}
5	*SKIV2L2*	36	54,639,332	54,757,166	7.97×10^{-4}
2	*GPR17*[b]	20	128,120,216	128,126,683	8.22×10^{-4}
2	*LIMS2*[b]	23	128,112,470	128,138,583	9.35×10^{-4}
1	*TSEN15*	33	182,287,433	182,309,967	9.80×10^{-4}

[a,b] The gene boundaries are overlapping as SNPs can be allocated to multiple genes, so the same SNP could be driving the signal in different genes. The results are ordered by significance.

(Alix and Domingues, 2011). Indeed, molecules involved in cell adhesions, namely, proinflammatory intracellular cell adhesion molecules that were used to examine the extent of ischemia-induced white matter lesions, were found to be significantly increased in white matter of subjects with major depressive disorder (Thomas et al., 2003). This functional evidence further lends weight to the importance of neuronal transmission and cell adhesion to white matter integrity.

The present study has a number of strengths. One is the use of a global measure of white matter tract integrity, derived by PCA from the 12 major tracts of interest. This general component captures the large proportion of the individual differences in white matter integrity that is shared among different tracts, thus capturing substantial variance of relevant neuroscientific information in a single variable. Such data reduction is necessary on the phenotypic side for comprehensive genome-wide analyses. Another is the unbiased genome-wide search in a large cohort for this type of phenotype. Furthermore, all the LBC1936 participants have a narrow age range, 72 to 74 years, which is important because some studies report age-related changes in the heritability to several brain traits, in particular, FA measures of cerebral white matter (Kochunov et al., 2011a).

The study also has limitations. Whereas the sample size of the LBC1936 (n = 535) is large for a brain imaging study, it is modest for genome-wide association (WTCCC, 2007). Other studies with a genome-wide association ap-

Table 3
The association of candidate genes, previously identified in the literature as associated with the brains' white matter measured by FA, to g_{FA} using a gene-based test

Chromosome	Gene	Study	Number of SNPs in gene	p-value
1	*DISC1*	Sprooten et al. (2011)	129	0.81
2	*ErbB4*	Zuliani et al. (2011)	339	0.57
5	*ADRB2*	Penke et al. (2010b)	34	0.042
8	*NRG1*	McIntosh et al. (2008)	282	0.87
8	*CLU*	Braskie et al. (2011)	39	0.62
11	*BDNF*	Chiang et al. (2011b)	29	0.55
11	*BACE1*	Hu et al. (2006)	18	0.60
13	*DAOA*	Hall et al. (2008)	35	0.34
15	D15S816 (*MCTP2*)	Kochunov et al. (2010)	106	0.18
17	*SLC6A4 (5-HTTLPR)*	Pacheco et al. (2009)	19	0.60
19	*APOE*	Heise et al. (2011) and Shen et al. (2010)	19	0.67
19	*TOMM40*	Shen et al. (2010)	19	0.69
22	*COMT*	McIntosh et al. (2007)	54	0.95

The results are ordered by chromosomal position. The references cited are the most recent citations for candidate gene associations with white matter as measured by FA in healthy cohorts.

proach in this field (Hibar et al., 2011b; Stein et al., 2010) and similar cohorts (Kramer et al., 2011) have reported interesting results without having genome-wide significance. The effect sizes reported here (~8%) are larger than those generally reported for single gene associations in genome-wide association studies of other complex traits, such as height (Lango Allen et al., 2010). However, our power calculations show that we have power to detect these effect sizes. Our findings may be a beneficiary of the "Winner's Curse"—true-positive results with potentially overestimated effect sizes (Zollner and Pritchard, 2007). This may indicate that the phenotype under investigation here, g_{FA}, may capture a less genetically complex trait than height, for example. Nevertheless, the results reported previously in our article need to be interpreted with caution because the suggested genetic findings may be false positive. The lack of replication of the candidate gene studies may to due to the age differences in study populations and the small sample size of the original LBC1936 pilot study. The majority of previous studies were small (n < 100) and conducted in young adults. Alternatively, our genetic data may not have tagged the causative genetic variant and missed the genetic association. As the biological pathway analysis and clustering of biologically similar pathways are a form of exploratory analysis, it is important that these results, in particular, should be interpreted with care. Several potential biases can exist in pathway analyses, such as gene size (Wang et al., 2010). The source data for the biological pathway analysis in this study were the gene-based VEGAS output, which does not show a bias toward larger gene sizes (Liu et al., 2010), illustrated here by the lack of strong gene-based significance of the large *ADAMTS18* gene despite a high single SNP significance level. Large gene sizes can bias toward brain-related pathways, as brain-expressed genes are significantly larger than other human genes (Raychaudhuri et al., 2010).

The limitations notwithstanding, the gold standard for determining whether the aforementioned results are true-positive findings is replication, and this is required for all aspects of this analysis as will be discussed. Large genetics studies, so-called mega meta-analyses, have been fruitful in identifying genes associated with medical, psychiatric, and behavioral traits. The key to discovering and verifying promising genetics associations is through large samples formed from collaborations of many individual studies. This approach has been successful on a brain phenotypic level measuring, for example, hippocampal volume in the ENIGMA network (Enhancing Neuroimaging Genetics through MetaAnalysis enigma.loni.ucla.edu) (Stein et al., in press), an ideal network to source replication of the findings presented here. However, it is not currently easy to compare directly white matter tractography results across research groups because many different techniques are used to track and segment white matter pathways. Should any of our single genetic associations and molecular pathways to g_{FA}

be validated, it will be important to investigate them for further associations with brain and cognitive traits (Chiang et al., 2009). Additional investigations into other brain imaging biomarkers, white matter hyperintensity load, premorbid tract integrity, and the effect of age-related change are also important follow-up considerations for the reported SNP associations.

5. Conclusion

This is the first genome-wide association study of brain white matter integrity. We report genome-wide suggestive hits for SNP, gene associations, and molecular pathways. These genes and pathways are now a target for future replication in larger cohorts. The identification of genetic influences involved in determining the integrity of the brain's white matter is one starting point for elucidating the biological mechanisms underlying brain connectivity.

Disclosure statement

None of the authors have any actual or potential conflicts of interest including any financial, personal, or other relationships with other people or organizations within 3 years of beginning the work submitted that could inappropriately influence (bias) their work. None of the institutions have contracts relating to this research through which it or any other organization may stand to gain financially now or in the future. None of the authors or institutions have any other agreements with authors or their institutions that could be seen as involving a financial interest in this work. The data contained in this manuscript have not been previously published, and all authors have reviewed the contents of the manuscript approved its contents, and validated the accuracy of the data.

Appendix A. Supplementary data

Supplementary data associated with this article can be found in the online version at doi: 10.1016/j.neurobiolaging. 2012.02.003.

References

Alix, J.J., Domingues, A.M., 2011. White matter synapses: form, function, and dysfunction. Neurology 76, 397–404.

Bastin, M.E., Maniega, S.M., Ferguson, K.J., Brown, L.J., Wardlaw, J.M., MacLullich, A.M.J., Clayden, J.D., 2010. Quantifying the effects of normal ageing on white matter structure using unsupervised tract shape modelling. Neuroimage 51, 1–10.

Beaulieu, C., 2002. The basis of anisotropic water diffusion in the nervous system—a technical review. NMR Biomed. 15, 435–455.

Behrens, T.E.J., Berg, H.J., Jbabdi, S., Rushworth, M.F.S., Woolrich, M.W., 2007. Probabilistic diffusion tractography with multiple fibre orientations: What can we gain? Neuroimage 34, 144–155.

Benjamini, Y., Hochberg, Y., 1995. Controlling the false discovery rate: a practical and powerful approach to multiple testing. J. R. Stat. Soc'Y B Stat. Methodol. 57, 289–300.

Braskie, M.N., Jahanshad, N., Stein, J.L., Barysheva, M., McMahon, K.L., de Zubicaray, G.I., Martin, N.G., Wright, M.J., Ringman, J.M., Toga, A.W., Thompson, P.M., 2011. Common Alzheimer's disease risk variant within the CLU gene affects white matter microstructure in young adults. J. Neurosci. 31, 6764–6770.

Chiang, M.C., Barysheva, M., Shattuck, D.W., Lee, A.D., Madsen, S.K., Avedissian, C., Klunder, A.D., Toga, A.W., McMahon, K.L., de Zubicaray, G.I., Wright, M.J., Srivastava, A., Balov, N., Thompson, P.M., 2009. Genetics of brain fiber architecture and intellectual performance. J. Neurosci. 29, 2212–2224.

Chiang, M.C., Barysheva, M., Toga, A.W., Medland, S.E., Hansel, N.K., James, M.R., McMahon, K.L., de Zubicaray, G.I., Martin, N.G., Wright, M.J., Thompson, P.M., 2011a. BDNF gene effects on brain circuitry replicated in 455 twins. Neuroimage 55, 448–454.

Chiang, M.C., McMahon, K.L., de Zubicaray, G.I., Martin, N.G., Hickie, I., Toga, A.W., Wright, M.J., Thompson, P.M., 2011b. Genetics of white matter development: a DTI study of 705 twins and their siblings aged 12 to 29. Neuroimage 54, 2308–2317.

Clayden, J.D., King, M.D., Clark, C.A., 2009a. Shape modelling for tract selection. Proceedings of the 12th International Conference on Medical Image Computing and Computer Assisted Intervention (MICCAI). Lecture Notes in Computer Science, 5762, 150–157.

Clayden, J.D., Storkey, A.J., Bastin, M.E., 2007. A Probabilistic model-based approach to consistent white matter tract segmentation. IEEE Trans. Med. Imaging 26, 1555–1561.

Clayden, J.D., Storkey, A.J., Maniega, S.M., Bastin, M.E., 2009b. Reproducibility of tract segmentation between sessions using an unsupervised modeling-based approach. Neuroimage 45, 377–385.

Davies, G., Tenesa, A., Payton, A., Yang, J., Harris, S.E., Liewald, D., Ke, X., Le Hellard, S., Christoforou, A., Luciano, M., McGhee, K., Lopez, L., Gow, A.J., Corley, J., Redmond, P., Fox, H.C., Haggarty, P.,

Whalley, L.J., McNeill, G., Goddard, M.E., Espeseth, T., Lundervold, A.J., Reinvang, I., Pickles, A., Steen, V.M., Ollier, W., Porteous, D.J., Horan, M., Starr, J.M., Pendleton, N., Visscher, P.M., Deary, I.J., 2011. Genome-wide association studies establish that human intelligence is highly heritable and polygenic. Mol. Psychiatry 16, 996–1005.

Deary, I.J., Gow, A.J., Taylor, M.D., Corley, J., Brett, C., Wilson, V., Campbell, H., Whalley, L.J., Visscher, P.M., Porteous, D.J., Starr, J.M., 2007. The Lothian Birth Cohort 1936: a study to examine influences on cognitive ageing from age 11 to age 70 and beyond. BMC Geriatr. 7, 28.

Deng, H.W., Xiong, D.H., Liu, X.G., Guo, Y.F., Tan, L.J., Wang, L., Sha, B.Y., Tang, Z.H., Pan, F., Yang, T.L., Chen, X.D., Lei, S.F., Yerges, L.M., Zhu, X.Z., Wheeler, V.W., Patrick, A.L., Bunker, C.H., Guo, Y., Yan, H., Pei, Y.F., Zhang, Y.P., Levy, S., Papasian, C.J., Xiao, P., Lundberg, Y.W., Recker, R.R., Liu, Y.Z., Liu, Y.J., Zmuda, J.M., 2009. Genome-wide association and follow-up replication studies identified ADAMTS18 and TGFBR3 as bone mass candidate genes in different ethnic groups. Am. J. Hum. Genet. 84, 388–398.

Duncan, D., Prodduturi, N., Zhang, B., 2010. WebGestalt2: an updated and expanded version of the Web-based Gene Set Analysis Toolkit. BMC Bioinform. 11, 10.

Folstein, M.F., Folstein, S.E., McHugh, P.R., 1975. Mini-mental state. A practical method for grading the cognitive state of patients for the clinician. J. Psychiatr. Res. 12, 189–198 [DOI: 10.1016/0022-3956(75)90026-6].

Ge, D., Zhang, K., Need, A.C., Martin, O., Fellay, J., Urban, T.J., Telenti, A., Goldstein, D.B., 2008. WGAViewer: software for genomic annotation of whole genome association studies. Genome Res. 18, 640–643.

Gilmore, J.H., Schmitt, J.E., Knickmeyer, R.C., Smith, J.K., Lin, W.L., Styner, M., Gerig, G., Neale, M.C., 2010. Genetic and environmental contributions to neonatal brain structure: a twin study. Hum. Brain Mapp. 31, 1174–1182.

Hall, J., Whalley, H.C., Moorhead, T.W., Baig, B.J., McIntosh, A.M., Job, D.E., Owens, D.G., Lawrie, S.M., Johnstone, E.C., 2008. Genetic variation in the DAOA (G72) gene modulates hippocampal function in subjects at high risk of schizophrenia. Biol. Psychiatry 64, 428–433.

Heinzen, E.L., Ge, D., Cronin, K.D., Maia, J.M., Shianna, K.V., Gabriel, W.N., Welsh-Bohmer, K.A., Hulette, C.M., Denny, T.N., Goldstein, D.B., 2008. Tissue-specific genetic control of splicing: implications for the study of complex traits. PLoS Biol. 6, e1.

Heise, V., Filippini, N., Ebmeier, K.P., Mackay, C.E., 2011. The APOE varepsilon4 allele modulates brain white matter integrity in healthy adults. Mol. Psychiatry 16, 908–916.

Hibar, D.P., Kohannim, O., Stein, J.L., Chiang, M.C., Thompson, P.M., 2011a. Multilocus genetic analysis of brain images. Front. Statical Genet. Methodol. 2, 1–11.

Hibar, D.P., Stein, J.L., Kohannim, O., Jahanshad, N., Saykin, A.J., Shen, L., Kim, S., Pankratz, N., Foroud, T., Huentelman, M.J., Potkin, S.G., Jack, C.R., Jr, Weiner, M.W., Toga, A.W., Thompson, P.M., 2011b. Voxelwise gene-wide association study (vGeneWAS): multivariate gene-based association testing in 731 elderly subjects. Neuroimage 56, 1875–1891.

Houlihan, L.M., Davies, G., Tenesa, A., Harris, S.E., Luciano, M., Gow, A.J., McGhee, K.A., Liewald, D.C., Porteous, D.J., Starr, J.M., Lowe, G.D., Visscher, P.M., Deary, I.J., 2010. Common variants of large effect in F12, KNG1, and HRG are associated with activated partial thromboplastin time. Am. J. Hum. Genet. 86, 626–631.

Hu, X., Hicks, C.W., He, W., Wong, P., Macklin, W.B., Trapp, B.D., Yan, R., 2006. Bace1 modulates myelination in the central and peripheral nervous system. Nat. Neurosci. 9, 1520–1525.

Huang, D.W., Sherman, B.T., Lempicki, R.A., 2009. Systematic and integrative analysis of large gene lists using DAVID bioinformatics resources. Nat. Protoc. 4, 44–57.

Jenkinson, M., Smith, S., 2001. A global optimisation method for robust affine registration of brain images. Med. Image Anal. 5, 143–156 [DOI: 10.1016/S1361-8415(01)00036-6].

Jin, H., Wang, X., Ying, J., Wong, A.H., Li, H., Lee, K.Y., Srivastava, G., Chan, A.T., Yeo, W., Ma, B.B., Putti, T.C., Lung, M.L., Shen, Z.Y., Xu, L.Y., Langford, C., Tao, Q., 2007. Epigenetic identification of ADAMTS18 as a novel 16q23.1 tumor suppressor frequently silenced in esophageal, nasopharyngeal and multiple other carcinomas. Oncogene 26, 7490–7498.

Jones, D.K., Williams, S.C., Gasston, D., Horsfield, M.A., Simmons, A., Howard, R., 2002. Isotropic resolution diffusion tensor imaging with whole brain acquisition in a clinically acceptable time. Hum. Brain Mapp. 15, 216–230.

Kent, W.J., Sugnet, C.W., Furey, T.S., Roskin, K.M., Pringle, T.H., Zahler, A.M., Haussler, D., 2002. The human genome browser at UCSC. Genome Res. 12, 996–1006.

Kochunov, P., Glahn, D.C., Lancaster, J., Thompson, P.M., Kochunov, V., Rogers, B., Fox, P., Blangero, J., Williamson, D.E., 2011a. Fractional anisotropy of cerebral white matter and thickness of cortical gray matter across the lifespan. Neuroimage 58, 41–49.

Kochunov, P., Glahn, D.C., Lancaster, J.L., Winkler, A.M., Smith, S., Thompson, P.M., Almasy, L., Duggirala, R., Fox, P.T., Blangero, J., 2010. Genetics of microstructure of cerebral white matter using diffusion tensor imaging. Neuroimage 53, 1109–1116.

Kochunov, P., Glahn, D.C., Nichols, T.E., Winkler, A.M., Hong, E.L., Holcomb, H.H., Stein, J.L., Thompson, P.M., Curran, J.E., Carless, M.A., Olvera, R.L., Johnson, M.P., Cole, S.A., Kochunov, V., Kent, J., Blangero, J., 2011b. Genetic analysis of cortical thickness and fractional anisotropy of water diffusion in the brain. Front. Neurosci. 5, 120.

Kramer, P.L., Xu, H., Woltjer, R.L., Westaway, S.K., Clark, D., Erten-Lyons, D., Kaye, J.A., Welsh-Bohmer, K.A., Troncoso, J.C., Markesbery, W.R., Petersen, R.C., Turner, R.S., Kukull, W.A., Bennett, D.A., Galasko, D., Morris, J.C., Ott, J., 2011. Alzheimer disease pathology in cognitively healthy elderly: a genome-wide study. Neurobiol. Aging 32, 2113–2122.

Kremen, W.S., Prom-Wormley, E., Panizzon, M.S., Eyler, L.T., Fischl, B., Neale, M.C., Franz, C.E., Lyons, M.J., Pacheco, J., Perry, M.E., Stevens, A., Schmitt, J.E., Grant, M.D., Seidman, L.J., Thermenos, H.W., Tsuang, M.T., Eisen, S.A., Dale, A.M., Fennema-Notestine, C., 2010. Genetic and environmental influences on the size of specific brain regions in midlife: The VETSA MRI study. Neuroimage 49, 1213–1223.

Lango Allen, H., Estrada, K., Lettre, G., Berndt, S.I., Weedon, M.N., Rivadeneira, F., Willer, C.J., Jackson, A.U., Vedantam, S., Raychaudhuri, S., Ferreira, T., Wood, A.R., Weyant, R.J., Segrè, A.V., Speliotes, E.K., Wheeler, E., Soranzo, N., Park, J.H., Yang, J., Gudbjartsson, D., Heard-Costa, N.L., Randall, J.C., Qi, L., Vernon Smith, A., Mägi, R., Pastinen, T., Liang, L., Heid, I.M., Luan, J., Thorleifsson, G., Winkler, T.W., Goddard, M.E., Sin Lo, K., Palmer, C., Workalemahu, T., Aulchenko, Y.S., Johansson, A., Zillikens, M.C., Feitosa, M.F., Esko, T., Johnson, T., Ketkar, S., Kraft, P., Mangino, M., Prokopenko, I., Absher, D., Albrecht, E., Ernst, F., Glazer, N.L., Hayward, C., Hottenga, J.J., Jacobs, K.B., Knowles, J.W., Kutalik, Z., Monda, K.L., Polasek, O., Preuss, M., Rayner, N.W., Robertson, N.R., Steinthorsdottir, V., Tyrer, J.P., Voight, B.F., Wiklund, F., Xu, J., Zhao, J.H., Nyholt, D.R., Pellikka, N., Perola, M., Perry, J.R., Surakka, I., Tammesoo, M.L., Altmaier, E.L., Amin, N., Aspelund, T., Bhangale, T., Boucher, G., Chasman, D.I., Chen, C., Coin, L., Cooper, M.N., Dixon, A.L., Gibson, Q., Grundberg, E., Hao, K., Juhani Junttila, M., Kaplan, L.M., Kettunen, J., Konig, I.R., Kwan, T., Lawrence, R.W., Levinson, D.F., Lorentzon, M., McKnight, B., Morris, A.P., Muller, M., Suh Ngwa, J., Purcell, S., Rafelt, S., Salem, R.M., Salvi, E., Sanna, S., Shi, J., Sovio, U., Thompson, J.R., Turchin, M.C., Vandenput, L., Verlaan, D.J., Vitart, V., White, C.C., Ziegler, A., Almgren, P., Balmforth, A.J., Campbell, H., Citterio, L., De Grandi, A., Dominiczak, A., Duan, J., Elliott, P., Elosua, R., Eriksson, J.G., Freimer, N.B., Geus, E.J., Glorioso, N., Haiqing, S., Hartikainen, A.L., Havulinna, A.S., Hicks, A.A., Hui, J., Igl, W., Illig, T., Jula, A., Kajantie, E., Kilpelainen, T.O., Koiranen, M., Kolcic, I., Koskinen, S., Kovacs, P., Laitinen, J., Liu, J., Lokki, M.L., Marusic, A., Maschio, A., Meitinger, T., Mulas, A., Pare, G., Parker, A.N., Peden, J.F., Petersmann, A., Pichler, I., Pietilainen, K.H., Pouta, A., Ridderstrale, M., Rotter, J.I., Sambrook, J.G., Sanders, A.R., Schmidt, C.O., Sinisalo, J., Smit, J.H., Stringham, H.M., Bragi Walters, G., Widen, E., Wild, S.H., Willemsen, G., Zagato, L., Zgaga, L., Zitting, P., Alavere, H., Farrall, M., McArdle, W.L., Nelis, M., Peters, M.J., Ripatti, S., van Meurs, J.B., Aben, K.K., Ardlie, K.G., Beckmann, J.S., Beilby, J.P., Bergman, R.N., Bergmann, S., Collins, F.S., Cusi, D., den Heijer, M., Eiriksdottir, G., Gejman, P.V., Hall, A.S., Hamsten, A., Huikuri, H.V., Iribarren, C., Kahonen, M., Kaprio, J., Kathiresan, S., Kiemeney, L., Kocher, T., Launer, L.J., Lehtimaki, T., Melander, O., Mosley, T.H., Jr, Musk, A.W., Nieminen, M.S., O'Donnell, C.J., Ohlsson, C., Oostra, B., Palmer, L.J., Raitakari, O., Ridker, P.M., Rioux, J.D., Rissanen, A., Rivolta, C., Schunkert, H., Shuldiner, A.R., Siscovick, D.S., Stumvoll, M., Tonjes, A., Tuomilehto, J., van Ommen, G.J., Viikari, J., Heath, A.C., Martin, N.G., Montgomery, G.W., Province, M.A., Kayser, M., Arnold, A.M., Atwood, L.D., Boerwinkle, E., Chanock, S.J., Deloukas, P., Gieger, C., Gronberg, H., Hall, P., Hattersley, A.T., Hengstenberg, C., Hoffman, W., Lathrop, G.M., Salomaa, V., Schreiber, S., Uda, M., Waterworth, D., Wright, A.F., Assimes, T.L., Barroso, I., Hofman, A., Mohlke, K.L., Boomsma, D.I., Caulfield, M.J., Cupples, L.A., Erdmann, J., Fox, C.S., Gudnason, V., Gyllensten, U., Harris, T.B., Hayes, R.B., Jarvelin, M.R., Mooser, V., Munroe, P.B., Ouwehand, W.H., Penninx, B.W., Pramstaller, P.P., Quertermous, T., Rudan, I., Samani, N.J., Spector, T.D., Volzke, H., Watkins, H., Wilson, J.F., Groop, L.C., Haritunians, T., Hu, F.B., Kaplan, R.C., Metspalu, A., North, K.E., Schlessinger, D., Wareham, N.J., Hunter, D.J., O'Connell, J.R., Strachan, D.P., Wichmann, H.E., Borecki, I.B., van Duijn, C.M., Schadt, E.E., Thorsteinsdottir, U., Peltonen, L., Uitterlinden, A.G., Visscher, P.M., Chatterjee, N., Loos, R.J., Boehnke, M., McCarthy, M.I., Ingelsson, E., Lindgren, C.M., Abecasis, G.R., Stefansson, K., Frayling, T.M., Hirschhorn, J.N., 2010. Hundreds of variants clustered in genomic loci and biological pathways affect human height. Nature 467, 832–838.

Li, Z., Nardi, M.A., Li, Y.S., Zhang, W., Pan, R., Dang, S., Yee, H., Quartermain, D., Jonas, S., Karpatkin, S., 2009. C-terminal ADAMTS-18 fragment induces oxidative platelet fragmentation, dissolves platelet aggregates, and protects against carotid artery occlusion and cerebral stroke. Blood 113, 6051–6060.

Liu, J.Z., McRae, A.F., Nyholt, D.R., Medland, S.E., Wray, N.R., Brown, K.M., Hayward, N.K., Montgomery, G.W., Visscher, P.M., Martin, N.G., Macgregor, S., 2010. A versatile gene-based test for genome-wide association studies. Am. J. Hum. Genet. 87, 139–145.

McIntosh, A.M., Baig, B.J., Hall, J., Job, D., Whalley, H.C., Lymer, G.K., Moorhead, T.W., Owens, D.G., Miller, P., Porteous, D., Lawrie, S.M., Johnstone, E.C., 2007. Relationship of catechol-*O*-methyltransferase variants to brain structure and function in a population at high risk of psychosis. Biol. Psychiatry 61, 1127–1134.

McIntosh, A.M., Moorhead, T.W., Job, D., Muñoz Maniega, G.K., Lymer, S., McKirdy, J., Sussmann, J.E., Baig, B.J., Bastin, M.E., Porteous, D., Evans, K.L., Johnstone, E.C., Lawrie, S.M., Hall, J., 2008. The effects of a neuregulin 1 variant on white matter density and integrity. Mol. Psychiatry 13, 1054–1059.

Muñoz Maniega, S.M., Bastin, M.E., McIntosh, A.M., Lawrie, S.M., Clayden, J.D., 2008. Atlas-based reference tracts improve automatic white matter segmentation with neighbourhood tractography. Proceedings of the 16th Scientific Meeting of the ISMRM, 3318.

Pacheco, J., Beevers, C.G., Benavides, C., McGeary, J., Stice, E., Schnyer, D.M., 2009. Frontal-limbic white matter pathway associations with the serotonin transporter gene promoter region (5-HTTLPR) polymorphism. J. Neurosci. 29, 6229–6233.

Penke, L., Maniega, S.M., Murray, C., Gow, A.J., Hernandez, M.C.V., Clayden, J.D., Starr, J.M., Wardlaw, J.M., Bastin, M.E., Deary, I.J., 2010a. A general factor of brain white matter integrity predicts information processing speed in healthy older people. J. Neurosci. 30, 7569–7574.

Penke, L., Munoz Maniega, S., Houlihan, L.M., Murray, C., Gow, A.J., Clayden, J.D., Bastin, M.E., Wardlaw, J.M., Deary, I.J., 2010b. White matter integrity in the splenium of the corpus callosum is related to successful cognitive aging and partly mediates the protective effect of an ancestral polymorphism in ADRB2. Behav. Genet. 40, 146–156.

Pfefferbaum, A., Sullivan, E.V., Carmelli, D., 2001. Genetic regulation of regional microstructure of the corpus callosum in late life. Neuroreport 12, 1677–1681.

Pruim, R.J., Welch, R.P., Sanna, S., Teslovich, T.M., Chines, P.S., Gliedt, T.P., Boehnke, M., Abecasis, G.R., Willer, C.J., 2010. LocusZoom: regional visualization of genome-wide association scan results. Bioinformatics 26, 2336–2337.

Purcell, S., Cherny, S.S., Sham, P.C., 2003. Genetic Power Calculator: design of linkage and association genetic mapping studies of complex traits. Bioinformatics 19, 149–150.

Purcell, S., Neale, B., Todd-Brown, K., Thomas, L., Ferreira, M.A.R., Bender, D., Maller, J., Sklar, P., de Bakker, P.I.W., Daly, M.J., Sham, P.C., 2007. PLINK: a tool set for whole-genome association and population-based linkage analyses. Am. J. Hum. Genet. 81, 559–575.

Raychaudhuri, S., Korn, J.M., McCarroll, S.A., Altshuler, D., Sklar, P., Purcell, S., Daly, M.J., 2010. Accurately assessing the risk of schizophrenia conferred by rare copy-number variation affecting genes with brain function. PLoS Genet. 6, pii: e1001097.

Rimol, L.M., Panizzon, M.S., Fennema-Notestine, C., Eyler, L.T., Fischl, B., Franz, C.E., Hagler, D.J., Lyons, M.J., Neale, M.C., Pacheco, J., Perry, M.E., Schmitt, J.E., Grant, M.D., Seidman, L.J., Thermenos, H.W., Tsuang, M.T., Eisen, S.A., Kremen, W.S., Dale, A.M., 2010. Cortical thickness is influenced by regionally specific genetic factors. Biol. Psychiatry 67, 493–499.

Schmitt, J.E., Wallace, G.L., Lenroot, R.K., Ordaz, S.E., Greenstein, D., Clasen, L., Kendler, K.S., Neale, M.C., Giedd, J.N., 2010. A twin study of intracerebral volumetric relationships. Behav. Genet. 40, 114–124.

Scottish Council for Research in Education. Mental Survey Committee, T.G., 1949. The Trend of Scottish Intelligence: a Comparison of the 1947 and 1932 Surveys of the Intelligence of Eleven-Year-Old Pupils. University of London Press, London.

Shen, L., Kim, S., Risacher, S.L., Nho, K., Swaminathan, S., West, J.D., Foroud, T., Pankratz, N., Moore, J.H., Sloan, C.D., Huentelman, M.J., Craig, D.W., DeChairo, B.M., Potkin, S.G., Jack, C.R., Weiner, M.W., Saykin, A.J., Initia, A.D.N., 2010. Whole genome association study of brain-wide imaging phenotypes for identifying quantitative trait loci in MCI and AD: a study of the ADNI cohort. Neuroimage 53, 1051–1063.

Smith, S.M., 2002. Fast robust automated brain extraction. Hum. Brain Mapp. 17, 143–155.

Sprooten, E., Sussmann, J.E., Moorhead, T.W., Whalley, H.C., Ffrench-Constant, C., Blumberg, H.P., Bastin, M.E., Hall, J., Lawrie, S.M., McIntosh, A.M., 2011. Association of white matter integrity with genetic variation in an exonic DISC1 SNP. Mol. Psychiatry 16, 8–9.

Stein, J.L., Hua, X., Morra, J.H., Lee, S., Hibar, D.P., Ho, A.J., Leow, A.D., Toga, A.W., Sul, J.H., Kang, H.M., Eskin, E., Saykin, A.J., Shen, L., Foroud, T., Pankratz, N., Huentelman, M.J., Craig, D.W., Gerber, J.D., Allen, A.N., Corneveaux, J.J., Stephan, D.A., Webster, J., De-Chairo, B.M., Potkin, S.G., Jack, C.R., Jr, Weiner, M.W., Thompson, P.M., Alzheimer's Disease Neuroimaging Initiative, 2010. Genome-wide analysis reveals novel genes influencing temporal lobe structure with relevance to neurodegeneration in Alzheimer's disease. Neuroimage 51, 542–554.

Stein, J.L., Medland, S.E., Arias Vasquez, A., Hibar, D.P., Senstad, R.E., Winkler, A.M., Toro, R., Appel, K., Bartecek, R., Bergmann, Ø., Bernard, M., Brown, A.A., Canon, D., Chakravarty, M., Christoforou, A., Domin, M., Grimm, O., Hollinshead, M., Holmes, A.J., Homuth, G., Hottenga, J.-J., Lopez, L.M., Hansell, N.K., Hwang, K.S., Kim, S., Laje, G., Lee, P.H., Liu, X., Loth, E., Lourdusamy, A., Muñoz Maniega, S., Mattingsdal, M., Nho, K., Nugent, A.C., O'Brien, C., Papmeyer, M., Pütz, B., Rijpkema, M., Risacher, S.L., Rose, E.J., Shen, L., Sprooten, E., Strengman, E., Teumer, A., van Eijk, K., van Erp, T.G.M., van Tol, M.-J., Wittfeld, K., Wolf, C., Woudstra, S., Aleman, A., Alhusaini, S., Almasy, L., Binder, E.B., Brohawn, D., Cantor, R.M., Carless, M.A., Corvin, A., Czisch, M., Curran, J.E., Davies, G., Delanty, N., Depondt, C., Duggirala, R., Dyer, T.D., Erk, S., Fagerness, J., Fox, P.T., Freimer, N.B., Gill, M., Göring, H.H.H., Höhn, D., Hosten, N., Johnson, M.P., Kasperaviciute, D., Kent, J., J.W., Kochunov, P., Lancaster, J.L., Lawrie, S.M., Liewald, D.C., Mandl, R., Matarin, M., Mattheisen, M., Meisenzahl, E., Melle, I., Moses, E.K., Mühleisen, T.W., Nauck, M., Nöthen, M.M., Olvera, R.L., Pike, G.B., Puls, R., Reinvang, I., Rentería, M.E., Rietschel, M., Roffman, J., Royle, N.A., Rujescu, D., Savitz, J., Schnack, H.G., Schnell, K., Steen, V.M., Valdés Hernández, M.C., Van den Heuvel, M., van der Wee, N.J., Van Haren, N.E.M., Veltman, J.A., Völzke, H., Walter, H., Agartz, I., Boomsma, D.I., Cavalleri, G.L., Dale, A.M., Djurovic, S., Drevets, W.C., Hagoort, P., Hall, J., Jack, J., C.R., Foroud, T.M., Le Hellard, S., Macciardi, F., Montgomery, G.W., Baptiste Poline, J., Porteous, D.J., Sisodiya, S.M., Starr, J.M., Sussmann, J., Toga, A.W., Veltman, D.J., Weiner, M.W., the Alzheimer's Disease Neuroimaging Initiative, IMAGEN Consortium, Saguenay Youth Study Group, Bis, J.C., Ikram, M.A., Smith, A.V., Tzourio, C., Vernooij, M.W., Launer, L.J., DeCarli, C., Seshadri, S., for the CHARGE Consortium, Andreassen, O.A., Apostolova, L.G., Bastin, M.E., Blangero, J., Brunner, H.G., Buckner, R.L., Cichon, S., Coppola, G., de Zubicaray, G.I., Deary, I.J., Donohoe, G., de Geus, E.J.C., Espeseth, T., Fernández, G., Glahn, D.C., Grabe, H.J., Jenkinson, M., Kahn, R.S., McDonald, C., McIntosh, A.M., McMahon, F.J., McMahon, K.L., Meyer-Lindenberg, A., Morris, D., Müller-Myhsok, B., Nichols, T.E., Ophoff, R.A., Paus, T., Pausova, Z., Penninx, B.W., Hulshoff Pol, H.E., Potkin, S.G., Sämann, P.G., Saykin, A.J., Schumann, G., Smoller, J.W., Wardlaw, J.M., Wright, M.J., Franke, B., Martin, N.G., Thompson, P.M., Consortium, E.N.G.t.M.-A.E, in press.Common genetic polymorphisms contribute to the variation in human hippocampal and intracranial volume. Nat. Genet.

Thomas, A.J., Perry, R., Kalaria, R.N., Oakley, A., McMeekin, W., O'Brien, J.T., 2003. Neuropathological evidence for ischemia in the white matter of the dorsolateral prefrontal cortex in late-life depression. Int. J. Geriatr. Psychiatry 18, 7–13.

Thompson, P.M., Martin, N.G., Wright, M.J., 2010. Imaging genomics. Curr. Opin. Neurol. 23, 368–373.

Wang, K., Li, M., Hakonarson, H., 2010. Analysing biological pathways in genome-wide association studies. Nat. Rev. Genet. 11, 843–854.

Wardlaw, J.M., Bastin, M.E., Valdes Hernandez, M.C., Munoz Maniega, S., Royle, N., Morris, Z., Clayden, J.D., Sandeman, E., Eadie, E., Murray, C., Starr, J.M., Deary, I.J., 2011. Brain ageing, cognition in youth and old age, and vascular disease in the Lothian Birth Cohort 1936: rationale, design and methodology of the imaging protocol. Int. J. Stroke 6, 547–559.

WTCCC, 2007. Genome-wide association study of 14,000 cases of seven common diseases and 3,000 shared controls. Nature 447, 661–678.

Zhang, B., Kirov, S., Snoddy, J., 2005. WebGestalt: an integrated system for exploring gene sets in various biological contexts. Nucleic Acids Res. 33, W741–W748.

Zollner, S., Pritchard, J.K., 2007. Overcoming the winner's curse: estimating penetrance parameters from case-control data. Am. J. Hum. Genet. 80, 605–615.

Zuliani, R., Moorhead, T.W., Bastin, M.E., Johnstone, E.C., Lawrie, S.M., Brambilla, P., O'Donovan, M.C., Owen, M.J., Hall, J., McIntosh, A.M., 2011. Genetic variants in the ErbB4 gene are associated with white matter integrity. Psychiatry Res. 191, 133–137.